Analysis of Two-Neutron ($L=0$) Transfer Cross Sections for Calcium and Nickel*

B. F. Bayman and Norton M. Hintz
School of Physics and Astronomy, University of Minnesota, Minneapolis, Minnesota 55455
(Received 12 February 1968)

We have tried to determine whether experimental data on $L=0$ (t,p) and (p,t) reactions on the even calcium and nickel isotopes are consistent with a reasonable amount of configuration mixing and a distorted-wave Born-approximation treatment of the two-neutron transfer process. Our calcium calculation involves the six shells from $2s_{1/2}$ through $1f_{5/2}$; our nickel calculation involves the five shells from $1f_{7/2}$ through $1g_{9/2}$. We have simulated the configuration mixing by diagonalizing a pairing force between seniority-zero states. The calculated eigenstates are consistent with one-particle transfer data, and give a satisfactory account of the ratios of observed (t,p) and (p,t) cross sections for ground-state transitions. However, certain excited calcium states seen in the (t,p) reaction are predicted to be populated with about twice the observed cross section. These states must involve more complicated degrees of freedom than the seniority-zero components we have included. Calculated (t,p) angular distributions are in good agreement with the experimental data. Calculated (p,t) angular distributions are about 5° out of phase with the experimental data.

I. INTRODUCTION

THIS paper describes a study of the systematics of zero angular momentum transfer (p,t) and (t,p) reactions in the even calcium and nickel isotopes. We confine our attention to the following experimental data:

(1) The (t,p) reaction on targets of $Ca^{40,42,44,46,48}$, leading to the ground states of the residual nuclei, and to excited 0^+ states at about 5.8 MeV.[1] The triton bombarding energy was 10–12 MeV.

(2) The (p,t) reaction on targets of $Ca^{40,42,48}$ and $Ni^{58,60,62,64}$ leading to the ground states of the residual nuclei.[2] The proton bombarding energy was 39.8 MeV.

Let us begin by assuming that the nuclear states involved have the simplest possible pure configurations. Then the ground state of Ca^{40} would be described in terms of closed proton and neutron shells. The $Ca^{42,44,46,48}$ ground states would have, in addition, neutrons in the $1f_{7/2}$ shell, and the Ca^{50} ground state would have two $2p_{3/2}$ neutrons outside a filled $1f_{7/2}$ neutron shell. Furthermore, the Ni^{56} ground state would also be described in terms of closed proton and neutron shells, whereas the ground states of Ni^{58} and Ni^{60} would have 2 or 4 extra neutrons in the $2p_{3/2}$ shell. When we consider Ni^{62} and Ni^{64}, we must also allow the ground states to contain $1f_{5/2}$ or $2p_{1/2}$ neutrons.

It has been noted[3] that these simple configurations imply (p,t) and (t,p) systematics that are in sharp conflict with the experimental data. According to distorted-wave Born-approximation (DWBA) treatments of the two-neutron transfer reaction as a direct process, the cross section for the transfer of a zero-coupled $2p_{3/2}$ pair is about six times[4] greater than the cross section for the transfer of a zero-coupled $1f_{7/2}$ pair (see Table X). The configurations described above imply that $Ni^{58}(p,t)Ni^{56}$ (ground state) involves pure $2p_{3/2}$ transfer. Thus if we assume pure configurations and ignore the effects on the cross section due to the differences in radii, optical parameters, Q values, etc., we would expect the ground-state $Ni^{58}(p,t)$ and $Ca^{42}(p,t)$ cross sections to be in the ratio of about 6:1. Actually it is 1.1:1. Similarly, we would expect the $Ca^{48}(t,p)Ca^{50}$ (ground-state) and $Ca^{46}(t,p)^{48}$ (ground-state) cross sections to be in the ratio of 6:1, whereas the observed ratio is 2.5:1. Furthermore, if the ground states of $Ca^{42,44,46,48}$ are reached by stripping in a zero-coupled $1f_{7/2}$ pair, we might expect to reach an excited state in each case by stripping in a zero-coupled $2p_{3/2}$ pair, and this should occur with about six times the cross section of the ground-state transition. One or two excited 0^+ states are seen to be strongly populated in these nuclei, but with summed cross sections only about equal to the cross section of the ground-state transition.

On the other hand, the pure-configuration picture is supported by the absence of a strongly populated excited state in the reaction $Ca^{48}(t,p)Ca^{50}$ [since the $(2p_{3/2})^2$ strength has gone into the ground-state transition]. Furthermore, the ratios of the cross sections of the $Ca^{40,42,44,46}(t,p)$ ground-state reactions, or of the $Ca^{42,44,48}(p,t)$ ground-state reactions, do not deviate greatly from $1:\frac{3}{2}:\frac{3}{2}:1$, the ratios that would be obtained if only the $(1f_{7/2})^n$ configurations were involved.

Our object in this study is to determine whether a reasonable amount of configuration mixing, combined with a DWBA calculation of the reaction-dependent effects, can account for these (p,t) and (t,p) systematics.

* Supported in part by the U. S. Atomic Energy Commission.
[1] J. H. Bjerregaard, Ole Hansen, O. Nathan, R. Chapman, S. Hinds, and R. Middleton, Nucl. Phys. **A103**, 33 (1967).
[2] G. Bassani, N. Hintz, and C. D. Kavaloski, Phys. Rev. **136**, B1006 (1964); G. Bassani, J. R. Maxwell, G. Reynolds, and N.M. Hintz, in *Proceedings of the International Conference on Nuclear Physics, Paris, 1964* (Editions du Centre National de la Recherche Scientifique, Paris, 1965).
[3] R. N. Glover and A. McGregor, Phys. Letters **24B**, 97 (1967).
[4] R. N. Glover and A. C. Douglas [Phys. Letters **25B**, 333 (1967)] have quoted a value of 63 for this $2p_{3/2}$-to-$1f_{7/2}$ ratio. This is in gross disagreement with our calculated value of about 6. Reference 3 quotes a calculated value of 8.5.

II. CALCULATION

We performed a simple type of shell-model calculation, and used the wave functions so obtained to calculate spectroscopic amplitudes for the two-neutron transfer reaction. We then used these amplitudes to calculate differential cross sections. We chose to include many configurations, but to keep the neutron-neutron force very simple. The active single-particle states were, for the Ca isotopes,

$$2s_{1/2},\ 1d_{3/2},\ 1f_{7/2},\ 2p_{3/2},\ 2p_{1/2},\ 1f_{5/2},$$

and for the Ni isotopes,

$$1f_{7/2},\ 2p_{3/2},\ 1f_{5/2},\ 2p_{1/2},\ 1g_{9/2}.$$

Thus, for example, a neutron configuration for Ca^{46} would be

$$(2s_{1/2})^{n_1}(1d_{3/2})^{n_2}(1f_{7/2})^{n_3}(2p_{3/2})^{n_4}(2p_{1/2})^{n_5}(1f_{5/2})^{n_6},\quad (n_1+n_2+n_3+n_4+n_5+n_6=12) \quad (1)$$

plus closed shells up to and including the $1d_{5/2}$ shell. The protons are regarded as filling inert closed shells, up to and including the $1d_{3/2}$ shell. They play no role in our calculation. Of course there are enormously many 0^+ states of type (1), far too many to be included in any available shell-model program. Thus we have made the further assumption that the neutron-neutron interaction is a simple pairing force.[5] This means that the two states

$$(2s_{1/2})^{n_1 v_1}(1d_{3/2})^{n_2 v_2}(1f_{7/2})^{n_3 v_3}(2p_{3/2})^{n_4 v_4}\times(2p_{1/2})^{n_5 v_5}(1f_{5/2})^{n_6 v_6}$$

and

$$(2s_{1/2})^{n_1' v_1'}(1d_{3/2})^{n_2' v_2'}(1f_{7/2})^{n_3' v_3'}(2p_{3/2})^{n_4' v_4'}\times(2p_{1/2})^{n_5' v_5'}(1f_{5/2})^{n_6' v_6'}$$

will be connected by the interaction only if all the seniorities v_α and v_α' are equal:

$$v_1=v_1',\quad v_2=v_2',\quad v_3=v_3',\quad v_4=v_4',\quad v_5=v_5',\quad v=v_6'.$$

In particular, one energy matrix (say for Ca^{46}) would refer only to states of the form

$$(2s_{1/2})^{2t_1,0}(1d_{3/2})^{2t_2,0}(1f_{7/2})^{2t_3,0}(2p_{3/2})^{2t_4,0}(2p_{1/2})^{2t_5,0}\times(1f_{5/2})^{2t_6,0},\quad (t_1+t_2+\cdots+t_6=6) \quad (2)$$

which may be said to have total seniority zero. The lowest eigenvector of this matrix yields the nuclear ground state. Other eigenvectors yield excited 0^+ states. It should be remembered that the total seniority-zero states (2) are not the most general 0^+ states. We could achieve total angular momentum zero by coupling each $(n_\alpha l_\alpha j_\alpha)$ group to a nonzero I_α, and then coupling all the I_α to zero. Our principal assumption is that there are some 0^+ states in Ca^{46} (including the ground state) whose properties can be understood in terms of the more limited set of states with total seniority zero. Auerbach[6] and Cohen *et al.*[7] have performed a shell-model calculation without making this assumption, but restricting the active neutrons to the $2p_{3/2}$, $1f_{5/2}$, and $2p_{1/2}$ shells. They found that total seniority-zero states generally accounted for more about 95% of the even Ni ground states.

The pairing force matrix elements between total seniority-zero states are very simple. Suppose $a_{m_\alpha}{}^{n_\alpha l_\alpha j_\alpha\dagger}$ is a neutron creation operator for the single-particle state $\psi_m{}^{n_\alpha l_\alpha j_\alpha}$. Define

$$A_\alpha{}^\dagger\equiv\frac{1}{\sqrt{2}}\sum_{m=-j_\alpha}^{j_\alpha}(j_\alpha j_\alpha m-m|00)a_{m_\alpha}{}^{n_\alpha l_\alpha j_\alpha\dagger}a_{-m_\alpha}{}^{n_\alpha l_\alpha j_\alpha\dagger}$$

$$=\frac{1}{\sqrt{\Omega_\alpha}}\sum_{m=1/2}^{j_\alpha}(-1)^{j_\alpha-m}a_m{}^{n_\alpha l_\alpha j_\alpha\dagger}a_{-m}{}^{n_\alpha l_\alpha j_\alpha\dagger}, \quad (3)$$

where

$$\Omega_\alpha\equiv j_\alpha+\tfrac{1}{2}. \quad (4)$$

Then the anticommutation relations obeyed by the $a_m{}^{n_\alpha l_\alpha j_\alpha\dagger}$ and $a_m{}^{n_\alpha l_\alpha j_\alpha}$ imply that[8]

$$[A_\alpha,A_\beta{}^+]=\delta_{\alpha,\beta}(1-N_\alpha/\Omega_\alpha), \quad (5)$$

where N_α is the operator that counts the number of neutrons in the $n_\alpha l_\alpha j_\alpha$ shell. It is easy to calculate from (5) that

$$\langle 0|(A_\alpha)^{t_\alpha}(A_\beta{}^\dagger)^{t_\beta}|0\rangle=\delta_{\alpha,\beta}\frac{t_\alpha!\Omega_\alpha!}{(\Omega_\alpha-t_\alpha)!\Omega_\alpha{}^{t_\alpha}}, \quad (6)$$

so that a normalized state of type (2) can be written

$$\Psi_{t_1\cdots t_6}=\prod_{\alpha=1}^{6}\left(\frac{\Omega_\alpha{}^{t_\alpha}(\Omega_\alpha-t_\alpha)!}{t_\alpha!\Omega_\alpha!}\right)^{1/2}(A_\alpha{}^\dagger)^{t_\alpha}|0\rangle. \quad (7)$$

The pairing force is just

$$Q=-G\sum_{\alpha,\beta=1}^{6}(\Omega_\alpha\Omega_\beta)^{1/2}A_\alpha{}^\dagger A_\beta, \quad (8)$$

where G determines the force strength. Then (5) and (6) imply that a diagonal matrix element of Q is

$$\langle\Psi_{t_1\cdots t_6}|Q|\Psi_{t_1\cdots t_6}\rangle=-G\sum_{\alpha=1}^{6}\Omega_\alpha\frac{\Omega_\alpha{}^{t_\alpha}(\Omega_\alpha-t_\alpha)!}{t_\alpha!\Omega_\alpha!}\times\langle 0|(A_\alpha)^{t_\alpha}A_\alpha{}^\dagger A_\alpha(A_\alpha{}^\dagger)^{t_\alpha}|0\rangle \quad (9a)$$

$$=-G\sum_{\alpha=1}^{6}t_\alpha(\Omega_\alpha-t_\alpha+1),$$

[5] Our spectroscopic calculation is thus similar to that described by A. K. Kerman, R. D. Lawson, and H. M. Macfarlane, Phys. Rev. **124**, 162 (1961).

[6] N. Auerbach, Phys. Rev. **163**, 1203 (1967).

[7] S. Cohen, R. D. Lawson, M. H. Macfarlane, S. P. Pandya, and M. Soga, Phys. Rev. **160**, 903 (1967).

[8] B. R. Mottelson, in *Lectures at the International School of Physics "Enrico Fermi," Course 15*, edited by G. Racah (Academic Press Inc., New York, 1960), p. 44.

whereas an off-diagonal element is

$$\langle\Psi_{t_1\cdots t_\alpha\cdots t_\beta\cdots t_6}|Q|\Psi_{t_1\cdots(t_\alpha+1)\cdots(t_\beta-1)\cdots t_6}\rangle = -G[(t_\alpha+1)(\Omega_\alpha-t_\alpha)t_\beta(\Omega_\beta-t_\beta+1)]^{1/2}. \quad (9b)$$

The single-particle energies used for the Ca isotopes are given in Table I. They were obtained, as far as possible, from energy-weighted averages of one-particle-transfer spectroscopic factors.[9] The single-particle energies for the Ni isotopes were taken to be $\epsilon_{1f_{7/2}}=-4.0$ MeV, $\epsilon_{2p_{3/2}}=0.0$ MeV, $\epsilon_{1f_{5/2}}=0.78$ MeV, $\epsilon_{2p_{1/2}}=1.08$ MeV, and $\epsilon_{1g_{9/2}}=4.0$ MeV. The $\epsilon_{2p_{3/2}}-\epsilon_{1f_{5/2}}-\epsilon_{2p_{1/2}}$ splittings were obtained by assuming that the lowest $\frac{3}{2}^-$, $\frac{5}{2}^-$, and $\frac{1}{2}^-$ states in Ni^{57} have pure single-particle character.

Perhaps the most direct experimental determination of the pairing force strength is afforded by odd-even mass differences, e.g., numbers of the form

$$\Delta_{6-7-8}\equiv M(Ca^{46})+M(Ca^{48})-2M(Ca^{47}), \quad (10)$$

where M is the atomic mass. The linear combination (10) is free of any linear dependence of the mass on neutron number. Thus much of the effect of the single-particle energies is absent from (10). To calculate (10) we must extend our considerations to the odd-neutron isotopes of Ca and Ni. A normalized seniority-one state with angular momentum J_γ and $2(t_1+\cdots+t_6)+1$ neutrons has the form

$$\Psi_{t_1\cdots t_6}{}^{j_\alpha,m}=\prod_{\alpha(\alpha\neq\gamma)}\left(\frac{\Omega_\alpha{}^{t_\alpha}(\Omega_\alpha-t_\alpha)!}{t_\alpha!\Omega_\alpha!}\right)^{1/2}(A_\alpha{}^\dagger)^{t_\alpha} \times\left(\frac{\Omega_\gamma{}^{t_\alpha}(\Omega_\gamma-1-t_\gamma)!}{t_\gamma!(\Omega_\gamma-1)!}\right)^{1/2}(A_\gamma{}^\dagger)^{t_\gamma}n_m{}^{j\gamma\dagger}|0\rangle. \quad (7')$$

The "blocking" effect of the odd $n_m{}^{j\gamma\dagger}$ neutron effectively reduces the pair degeneracy Ω_γ by 1. Thus the matrix elements corresponding to (9a) and (9b) are simply obtained by replacing Ω_γ by $\Omega_\gamma-1$ in those expressions.

We found that $G=20/A$ MeV gives a reasonable representation of the odd-even mass differences (Table II). Because of the crudeness of our model, we have not thought it worthwhile to vary G from nucleus to nucleus, apart from the usual $1/A$ dependence.

TABLE I. Assumed single-particle energies for the calcium isotopes in MeV.

A \ State	$1f_{5/2}$	$2p_{1/2}$	$2p_{3/2}$	$1f_{7/2}$	$1d_{3/2}$	$2s_{1/2}$
40	−2.1	−4.07	−6.13	− 8.65	−15.16	−17.5
41	−1.9	−3.89	−5.94	− 8.75	−14.38	−16.85
42	−1.7	−3.1	−5.74	− 8.85	−13.6	−16.2
43	−1.6	−3.59	−5.59	− 9.07	−12.92	−15.6
44	−1.5	−3.48	−5.44	− 9.28	−12.24	−15.0
45	−1.4	−3.37	−5.29	− 9.45	−12.29	−14.4
46	−1.3	−3.26	−5.13	− 9.62	−12.33	−13.8
47	−1.25	−3.19	−5.15	− 9.78	−12.43	−13.18
48	−1.2	−3.12	−5.17	− 9.94	−12.52	−12.55
49	−1.15	−3.06	−5.19	−10.07	−12.61	−11.97
50	−1.1	−3.0	−5.2	−10.2	−12.7	−11.44

[9] Ole Hansen (private communication).

TABLE II. Experimental and calculated odd-even mass differences in MeV. The calculations used $G=20/A$.

	Expt	Calc		Expt	Calc
$Ca^{40}+Ca^{42}-2Ca^{41}$	3.14	3.13	$Ni^{56}+Ni^{58}-2Ni^{57}$	1.94	2.28
$Ca^{42}+Ca^{44}-2Ca^{43}$	3.21	3.25	$Ni^{58}+Ni^{60}-2Ni^{59}$	2.38	2.37
$Ca^{44}+Ca^{46}-2Ca^{45}$	2.98	3.08	$Ni^{60}+Ni^{62}-2Ni^{61}$	2.78	2.67
$Ca^{46}+Ca^{48}-2Ca^{47}$	2.66	2.93	$Ni^{62}+Ni^{64}-2Ni^{63}$	2.82	2.58
$Ca^{48}+Ca^{50}-2Ca^{49}$	1.57	1.47			

By restricting ourselves to states of seniority zero or seniority one, we have enormously reduced the sizes of the matrices we must diagonalize. However, they are still large. For example, in the case of Ca^{46} there are 119 seniority-zero states (2). We do not believe that they all play a significant role in the low-lying 0^+ states of Ca^{46}. To save time, we have included no more than 30 states of type (2), choosing these to be the 30 states with lowest summed single-particle energies. Thus we did not diagonalize matrices greater than 30×30.[10]

The diagonalization of the energy matrices yielded eigenvectors $C_{t_1\cdots t_6}$ for the Ca isotopes, or $C_{t_1\cdots t_5}$ for the Ni isotopes. Again using the case of Ca^{46} for illustration, the corresponding ground-state wave function has the form

$$\Psi(Ca^{46}\text{g.s.})=\sum_{\substack{t_1\cdots t_6\\(t_1+\cdots+t_6=6)}}C_{t_1\cdots t_6}\times\prod_{\alpha=1}^{6}\left(\frac{\Omega_\alpha{}^{t_\alpha}(\Omega_\alpha-t_\alpha)!}{t_\alpha!\Omega_\alpha!}\right)^{1/2}(A_\alpha{}^\dagger)^{t_\alpha}|0\rangle. \quad (11)$$

Tables III, IV, and V list the average occupation numbers N_α:

$$N_\alpha\equiv\sum_{t_1\cdots t_6}2t_\alpha[C_{t_1\cdots t_6}]^2, \quad (12)$$

calculated from the eigenvectors corresponding to the even Ca and Ni ground states, and the Ca excited states populated strongly in the (t,p) reaction. We include them here to convey a rough impression of the amount of configuration mixing implied by our eigenvectors.

TABLE III. Calculated average occupation numbers for the ground states of the even calcium isotopes. $G=20/A$.

Nucleus \ State	$1f_{5/2}$	$2p_{1/2}$	$2p_{3/2}$	$1f_{7/2}$	$1d_{3/2}$	$2s_{1/2}$
Ca^{40}	0.01	0.01	0.02	0.06	3.92	1.98
Ca^{42}	0.05	0.03	0.11	1.98	3.86	1.97
Ca^{44}	0.06	0.04	0.15	4.01	3.78	1.96
Ca^{46}	0.06	0.03	0.13	5.95	3.87	1.96
Ca^{48}	0.04	0.02	0.10	7.88	3.97	1.99
Ca^{50}	0.09	0.07	1.97	7.92	3.98	1.99

[10] All the numerical calculations in this study were performed on the CDC 6600 computer of the University of Minnesota Numerical Analysis Center.

TABLE IV. Calculated average occupation numbers for some excited states of even calcium isotopes. $G=20/A$.

Nucleus \ State	$1f_{5/2}$	$2p_{1/2}$	$2p_{3/2}$	$1f_{7/2}$	$1d_{3/2}$	$2s_{1/2}$
Ca^{42}	0.04	0.04	1.84	0.20	3.91	1.98
Ca^{44}	0.06	0.05	1.86	2.26	3.80	1.98
Ca^{46}	0.06	0.06	1.88	4.19	3.84	1.97
Ca^{48}	0.08	0.07	1.90	6.10	3.91	1.95
Ca^{50}	0.11	1.85	0.13	7.94	3.99	1.99

TABLE V. Calculated average occupation numbers for the ground states of the even nickel isotopes. $G=20/A$.

Nucleus \ State	$1g_{9/2}$	$2p_{1/2}$	$1f_{5/2}$	$2p_{3/2}$	$1f_{7/2}$
Ni^{56}	0.06	0.03	0.10	0.10	7.71
Ni^{58}	0.18	0.13	1.11	0.84	7.85
Ni^{60}	0.26	0.34	1.39	2.22	7.77
Ni^{62}	0.32	0.58	2.39	2.87	7.83
Ni^{64}	0.40	0.88	3.52	3.32	7.87

The ground-state occupation numbers N_α obtained in this calculation can be compared with summed spectroscopic factors $S_{\beta\alpha}$ from single-nucleon transfer

$$\sum_\beta (2j_\alpha+1)S_{\beta\alpha}=2j_\alpha+1-N_\alpha, \quad \text{for stripping}$$

$$\sum_\beta S_{\beta\alpha}=N_\alpha, \quad \text{for pickup}$$

where the β sums are over all final states reached by transfering a neutron in the single-particle state α. Unfortunately, the extraction of single-nucleon spectroscopic factors is still beset by a number of uncertainties. For example, Glasshauser, Rickey, and Rost[11] have observed $f_{7/2}$ neutron pickup from Ca^{40}. Their estimate of the spectroscopic factor varies from 0.14 to 0.28 depending upon the prescription used for determining the tail of the bound $f_{7/2}$ wave function. Furthermore, it is usually difficult to be certain that one has seen all the strength corresponding to a given (nlj) transfer. Thus, stripping data usually determine only an upper limit and pickup a lower limit to N_α. We have surveyed the recent literature on single-particle transfer and have extracted estimates of N_α to compare with the values given in Tables IV and V for the Ca and Ni isotopes. The comparisons, using $V_{j_\alpha}{}^2\equiv N_\alpha/(2j_\alpha+1)$, are shown in Figs. 1 and 2, where the theoretical $V_j{}^2$ are shown as histograms and the experimental values as points with estimated errors. Experimental references are given in the figure captions. We have not attempted an exhaustive and critical survey nor have we reanalyzed the authors data in a consistent over-all manner. The experimental $V_j{}^2$ are rather inaccurate for $V_j{}^2$ near zero in stripping, or near unity in pickup, due to over-all normalization uncertainties. Bearing the many difficulties in mind, the single-nucleon trans-

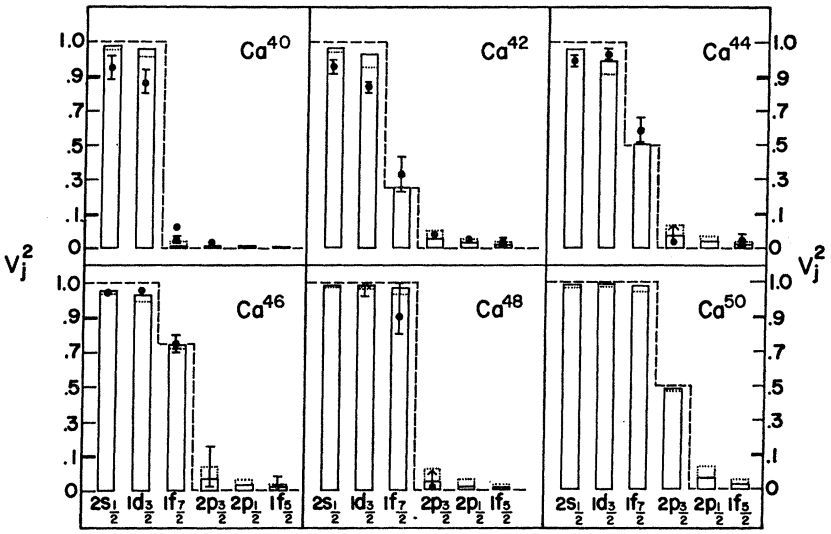

FIG. 1. Average ground-state occupation probabilities $V_j{}^2$ for the Ca isotopes for single-particle states indicated. Note expanded scale near zero and one. Rectangular bars are results of pairing force calculations presented in this paper for $G=20/A$. Dotted lines are for $G=27/A$. Dashed lines show unperturbed shell-model values. Solid black points are experimental values of $V_j{}^2$ derived from single-nucleon transfer data. Error bars, where shown, are only rough estimates of uncertainties or discrepancies. Arrows indicate the point shown is only a limit. Papers from which $V_j{}^2$ values were obtained are for Ca^{40}, T. Belote *et al.*, Phys. Rev. **139**, B80 (1965); R. Bock *et al.*, Phys. Letters **18**, 61 (1965); U. Lynan *et al.*, *ibid.* **25B**, 9 (1967); and C. Glashauser *et al.*, *ibid.* **14**, 113 (1965); for Ca^{42}, W. Dorenbusch *et al.*, Phys. Rev. **146**, 734 (1966); and U. Lynan *et al.*, Phys. Letters **25B**, 9 (1967); for Ca^{44}, J. Rapaport *et al.*, Phys. Rev. **156**, 1255 (1967); T. Conlon *et al.*, *ibid.* **144**, 941 (1966); and W. R. Smith *et al.*, Bull. Am. Phys. Soc. **12**, 93 (1967); for Ca^{46}, T. Belote *et al.*, Phys. Rev. **142**, 624 (1966); J. M. Bjerregaard *et al.*, *ibid.* **160**, 889 (1967); **138**, B1097 (1965); for Ca^{48}, T. Conlon *et al.*, *ibid.* **144**, 941 (1966); E. Kashy *et al.*, *ibid.* **135**, B865 (1964); and R. J. Peterson (to be published).

[11] C. Glashauser, M. Kondo, M. E. Rickey, and E. Rost, Phys. Letters **14**, 113 (1965).

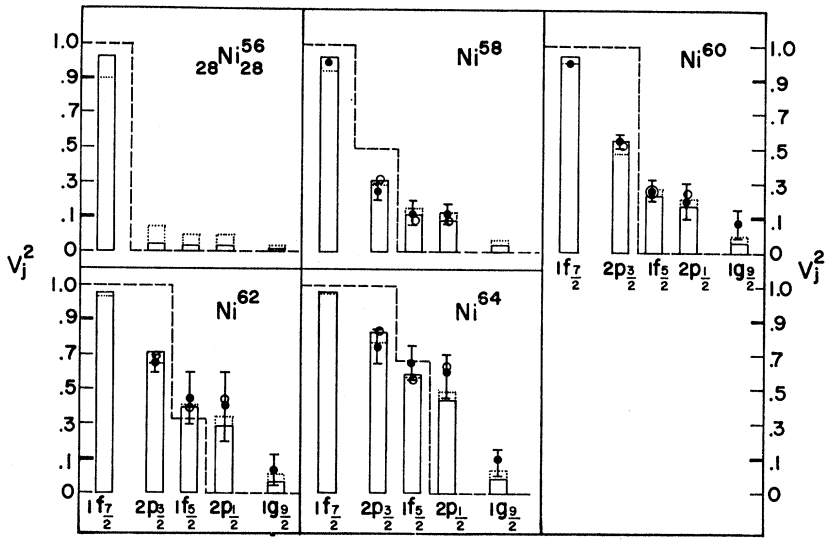

FIG. 2. Average ground-state occupation probabilities V_j^2 for the Ni isotopes for single-particle states indicated. Note expanded scale near zero and 1. Rectangular bars are results of pairing force calculations presented in this paper for $G=20/A$. Dotted lines are for $G=27/A$. Open circles are calculated V_j^2 from Cohen *et al.*, Ref. 7. Dashed lines show unperturbed shell-model values. Solid black points are experimental values of V_j^2 derived from single-nucleon transfer data. Error bars, where shown, are only rough estimates of uncertainties or discrepancies. Papers from which V_j^2 values were obtained are C. Fulmer *et al.*, Phys. Rev. **131**, 2133 (1964); **133**, B955 (1964); **139**, B579 (1965); E. Cosman *et al.*, *ibid.* **142**, 673 (1966); **163**, 1134 (1967); C. Fou *et al.*, *ibid.* **140**, B1283 (1965); **144**, 927 (1966).

fer data certainly seem consistent with the V_j^2 calculated here.

The Ni calculations of Auerbach[6] and Cohen *et al.*[7] also predict values of V_j^2. We have plotted in Fig. 2 the V_j^2 of Cohen *et al.* (Auerbach's values are very nearly the same).

The spectroscopic amplitude for the transfer of a j_β^2 zero-coupled pair between two states (say the Ca^{46} and Ca^{48} ground states) is expressed in terms of the eigenvector components as

$$
\begin{aligned}
&S_\beta(\mathrm{Ca}^{46}\text{g.s.} \leftrightarrow \mathrm{Ca}^{48}\text{g.s.}) \\
&= \langle \psi^\dagger(\mathrm{Ca}^{48}\text{g.s.}) A_\beta^\dagger \psi(\mathrm{Ca}^{46}\text{g.s.}) \rangle \\
&= \sum_{\substack{t_1 \cdots t_6 \\ (t_1+\cdots+t_6=6)}} D_{t_1 t_2 \cdots t_\beta+1 \cdots t_6} C_{t_1 t_2 \cdots t_\beta \cdots t_6} \\
&\quad \times \left(\frac{\Omega_\beta^{t_\beta+1} (\Omega_\beta - t_\beta + 1)! \, \Omega_\beta^{t_\beta} (\Omega_\beta - t_\beta)!}{(t_\beta+1)! \, \Omega_\beta! \, t_\beta! \, \Omega_\beta!} \right)^{1/2} \\
&\quad \times \langle 0 | (A_\beta)^{t_\beta+1} A_\beta^\dagger (A_\beta^\dagger)^{t_\beta} | 0 \rangle \\
&= \sum_{\substack{t_1 \cdots t_6 \\ (t_1+\cdots+t_6=6)}} D_{t_1 t_2 \cdots t_\beta+1 \cdots t_6} C_{t_1 \cdots t_\beta \cdots t_6} \\
&\quad \times \left(\frac{(t_\beta+1)(\Omega_\beta - t_\beta)}{\Omega_\beta} \right)^{1/2} . \qquad (13)
\end{aligned}
$$

The calculated amplitudes are listed in Tables VI, VII, and VIII.

This completes the spectroscopic part of the calculation. The spectroscopic amplitudes (13) were then used to calculate form factors $F_0(r)$ for the two-neutron

TABLE VI. Calculated two-neutron spectroscopic amplitudes for the ground states of the even calcium isotopes. $G=20/A$.

Reaction \ State	$1f_{5/2}$	$2p_{1/2}$	$2p_{3/2}$	$1f_{7/2}$	$1d_{3/2}$	$2s_{1/2}$
$Ca^{40} \leftrightarrow Ca^{42}$	0.14	0.11	0.22	0.97	0.18	0.09
$Ca^{42} \leftrightarrow Ca^{44}$	0.15	0.12	0.25	1.20	0.24	0.11
$Ca^{44} \leftrightarrow Ca^{46}$	0.16	0.12	0.24	1.20	0.31	0.12
$Ca^{46} \leftrightarrow Ca^{48}$	0.13	0.10	0.21	0.99	0.23	0.12
$Ca^{48} \leftrightarrow Ca^{50}$	0.18	0.17	0.98	0.22	0.10	0.07

TABLE VII. Calculated two-neutron spectroscopic amplitudes for (t,p) excitation of some excited states of even calcium isotopes. $G=20/A$.

Reaction \ State	$1f_{5/2}$	$2p_{1/2}$	$2p_{3/2}$	$1f_{7/2}$	$1d_{3/2}$	$2s_{1/2}$
$Ca^{40} \rightarrow Ca^{42*}$	0.12	0.12	0.95	−0.23	0.05	0.03
$Ca^{42} \rightarrow Ca^{44*}$	0.12	0.13	0.94	−0.09	0.06	0.03
$Ca^{44} \rightarrow Ca^{46*}$	0.13	0.15	0.94	0.02	0.08	0.04
$Ca^{46} \rightarrow Ca^{48*}$	0.16	0.16	0.95	0.09	0.08	0.05
$Ca^{48} \rightarrow Ca^{50*}$	0.20	0.95	−0.18	0.07	0.04	0.03

TABLE VIII. Calculated two-neutron spectroscopic amplitudes for the ground states of the even nickel isotopes. $G=20/A$.

Reaction \ State	$1g_{9/2}$	$2p_{1/2}$	$1f_{5/2}$	$2p_{3/2}$	$1f_{7/2}$
$Ni^{56} \leftrightarrow Ni^{58}$	0.28	0.29	0.57	0.77	0.36
$Ni^{58} \leftrightarrow Ni^{60}$	0.35	0.39	0.78	0.87	0.36
$Ni^{60} \leftrightarrow Ni^{62}$	0.39	0.49	0.95	0.79	0.32
$Ni^{62} \leftrightarrow Ni^{64}$	0.43	0.56	1.03	0.68	0.27

transfer reaction:

$$F_0(R)^{\mathrm{Ca}^{46}\mathrm{g.s.}\leftrightarrow\mathrm{Ca}^{48}\mathrm{g.s.}}=R\sum_{\alpha=1}^{6}S_\alpha(\mathrm{Ca}^{46}\mathrm{g.s.}\leftrightarrow\mathrm{Ca}^{48}\mathrm{g.s.})$$
$$\times((l_\alpha\tfrac{1}{2})_{j_\alpha}(l_\alpha\tfrac{1}{2})_{j_\alpha}|(l_\alpha l_\alpha)_0(\tfrac{1}{2}\ \tfrac{1}{2})_0)_0\int d\mathbf{r}\,e^{-(3/2)\kappa^2r^2}$$
$$\times u_{n_\alpha l_\alpha j_\alpha}(r_1)u_{n_\alpha l_\alpha j_\alpha}(r_2)[Y^{l_\alpha}(\hat{r}_1)Y^{l_\alpha}(\hat{r}_2)]_0{}^0. \quad (14)$$

The vectors $\mathbf{r}_1$ and $\mathbf{r}_2$ that occur in (14) are related to $\mathbf{R}$ and the integration variable $\mathbf{r}$ by

$$\mathbf{r}_1=\mathbf{R}-\tfrac{1}{2}\mathbf{r},\quad \mathbf{r}_2=\mathbf{R}+\tfrac{1}{2}\mathbf{r}. \quad (15)$$

The technique for performing integrals of this type, with arbitrary single-particle functions $u_{nlj}(r)$, is described in Ref. 12. We have taken the u_{nlj} to be single-particle eigenfunctions[13] in a Wood-Saxon well:

$$V(r)=V_0\left[\frac{1}{1+\exp[(r-r_0)/a_0]}+\lambda\frac{\hbar^2}{4m_\pi{}^2c^2}\right.$$
$$\left.\times\frac{\exp[(r-r_0)/a_0]}{\{1+\exp[(r-r_0)/a_0]\}^2a_0r}\times\begin{Bmatrix} l \\ -l-1\end{Bmatrix}\right]$$
$$\text{for}\quad j=\begin{Bmatrix} l+\frac{1}{2} \\ l-\frac{1}{2}\end{Bmatrix}, \quad (16)$$

with $r_0=1.25A^{1/3}$ F, $a_0=0.65$ F, and $\lambda=25.0$. The strength V_0 was adjusted in each case so that the eigenvalue ϵ associated with u_{nlj} was half the two-neutron separation energy, e.g., for the cases $\mathrm{Ca}^{46}(t,p)\mathrm{Ca}^{48\mathrm{g.s.}}$ or $\mathrm{Ca}^{48}(p,t)\mathrm{Ca}^{46\mathrm{g.s.}}$, this would be

$$\epsilon=-17.22/2\ \mathrm{MeV}=-8.61\ \mathrm{MeV}. \quad (17)$$

Note that a different V_0 was used for each $u_{n_\alpha l_\alpha j_\alpha}$ in (14), so that the eigenvalue always came to be equal to ϵ of (17). This ensured that the asymptotic part of the form factor (14) had the correct logarithmic derivative. Nevertheless, the procedure is somewhat arbitrary from the point of view of the shell model.

The basic assumption involved in (14) is that the interaction responsible for the reaction is a spin-independent δ function of the distance between the proton and the mass center of the two transferred neutrons. The orbital part of the triton wave fuuction was assumed to be

$$e^{-\kappa^2[(\mathbf{r}_1-\mathbf{r}_p)^2+(\mathbf{r}_2-\mathbf{r}_p)^2+(\mathbf{r}_1-\mathbf{r}_2)^2]}. \quad (18)$$

If the triton is to have its measured mean square radius of $(1.7\ \mathrm{F})^2$, then κ should have the value

$$\kappa=1/\sqrt{6}\times1.7\ \mathrm{F}=0.24\ \mathrm{F}^{-1}.$$

The jj-LS transformation amplitude in (12) expresses the assumed spin independence of the interaction, so that the process only occurs when transferred neutrons are in the singlet state, as they are in the triton whose orbital wave function is given by (18).

The form factor (14) was then inserted into a zero-range DWBA code, which calculated differential cross sections for the (t,p) and (p,t) reactions. We are grateful to W. R. Smith for supplying us with a copy of his (d,p) code,[14] which we were able to adapt for our purposes. The optical parameters used for the proton and triton channels were determined, as far as possible, from fits to elastic scattering data.[15] These parameters are listed in Table IX. All our calculated cross sections should be multiplied by a single normalization factor, which we have not attempted to calculate. If our calculation is successful, a suitable choice for this normalization factor should suffice for all the angular distributions, for all the target nuclei, and for all the final states.

It is perhaps useful to indicate the relative calculated cross sections associated with pure $(nlj)^2$ transfer. These numbers are given in Table X. The dominance of σ_{2p} over σ_{1f} is due to two factors:

(1) With a reasonably sized triton of the type (18), transfer is most probable when the two neutrons have a nodeless, relative s-state wave function. This is more likely for $(2p)_{L=0}{}^2$ than for $(1f)_{L=0}{}^2$.

(2) The radial node in the single-particle $2p$ wave function, and the higher centrifugal barrier seen by the $1f$ wave function, cause the $2p$ wave function to be larger in the region just beyond the nuclear surface, where the reaction takes place.

Note that $\sigma_{1f_{7/2}}>\sigma_{1f_{5/2}}$ and $\sigma_{2p_{3/2}}>\sigma_{2p_{1/2}}$. This is because of the following:

(1) The jj-LS transformation amplitude needed in (14) is greater when $j=l+\frac{1}{2}$ than when $j=l-\frac{1}{2}$ [in the ratio $[(l+1)/l]^{1/2}$.

(2) The spin-orbit part of the potential (16) seen by the bound neutrons was assumed to peak on the nuclear surface. This has the consequence that a $j=l+\frac{1}{2}$ neutron sees a slightly larger well than the corresponding $j=l-\frac{1}{2}$ neutron. The $j=l+\frac{1}{2}$ radial wave function is larger where the optical wave functions are larger.

The Q dependence of the cross section is determined by two competing effects. The $\mathrm{Ca}^{42}(p,t)$ reaction has a larger negative Q than the $\mathrm{Ca}^{48}(p,t)$ reaction. This means that the tritons leaving Ca^{42} are slower, and the momentum mismatch between the incoming proton and outgoing triton is smaller (if $E_p=39.8$ MeV). In the case of an $L=0$ transition, this smaller momentum mismatch generally leads to a larger cross section. On the other hand, the larger negative Q in Ca^{42} means that the

[12] B. F. Bayman and A. Kallio, Phys. Rev. **156**, 1121 (1967).

[13] We wish to thank E. Rost for sending us a computer program that calculates these eigenfunctions.

[14] W. R. Smith, Phys. Rev. **137**, B913 (1965).

[15] J. C. Hafele, E. R. Flynn, and A. G. Blair, Phys. Rev. **155**, 1238 (1967); F. Perey, *ibid.* **131**, 745 (1963); L. N. Blumberg, E. E. Gross, A. van der Woude, A. Zucker, and R. H. Bassel, *ibid.* **147**, 812 (1966).

TABLE IX. Optical parameters used in the DWBA calculation.

	Proton potentials								
				Volume			Surface		
E_{proton} (target)	r_0	a_0	V	r_0'	a_0'	W_V	r_0'	a_0'	W_S
~22 MeV (Ca)	1.25	0.65	53.0	...	...	...	1.25	0.47	15.5
39.8 MeV (Ca)	1.18	0.7	43.3	1.3	0.6	2.0	1.3	0.6	5.0
39.8 MeV (Ca)	1.18	0.7	44.7	1.3	0.6	7.1	1.3	0.6	2.3
	Triton potentials								
				Volume			Surface		
E_{triton} (target)	r_0	a_0	V	r_0'	a_0'	W_V	r_0'	a_0'	W_S
12 MeV (Ca)	1.24	0.678	144.0	1.45	0.841	30.0	...	...	...
~30 MeV (Ca)	1.24	0.678	146.0	1.45	0.841	25.1	...	...	...
~30 MeV (Ca)	1.24	0.678	153.0	1.45	0.841	24.7	...	...	...

single-neutron radial functions were assumed to be more tightly bound there, which acts to decrease the radial functions and form factors in the region of the nuclear surface, and thus the (p,t) cross section. It is seen from Table X that the net result of these competing effects is different for the different nlj. However, a general inference from the numbers in Table X is that σ_{nlj} for nlj in the same major shell seem to vary in the same way.

In comparing cross sections for different nuclei, one also encounters effects on the optical wave functions due to changes in the target charge and radius and optical parameters. According to our calculation these result in Ni^{58} σ_{nlj} that are about one-half to one-third of the corresponding Ca^{42} σ_{nlj}. This accounts for part of the discrepancy between the observed $Ni^{58}(p,t)$ to $Ca^{42}(p,t)$ ratio of 1.1, and the naively expected ratio of 6.

III. ANGULAR DISTRIBUTIONS

In Fig. 3 we show a comparison between experimental and calculated angular distributions for the $Ca(t,p)$ reactions. Each calculated curve is separately normalized to the corresponding set of data points so as to produce the best visual fit. It is evident that the observed angular distributions are very well reproduced by the theory. Indeed the fits are better than one could reasonably expect from a theory that makes such a crude assumption about the mechanism responsible for the reaction.

Figures 4 and 5 show similar comparisons between experimental and calculated angular distributions for the (p,t) reactions with 39.8-MeV incident protons. Here the agreement between theory and experiment is much poorer. In particular, the first minimum in the angular distribution is calculated to occur at about 15°, rather than at the observed angle of 10°. If a lower radial cutoff of 3.3 F is used in the DWBA integral, the calculated minimum is brought in to about 10°. Use of a lower radial cutoff introduces an additional parameter into the calculation, a parameter which affects the relative cross sections for the different targets. We have not used a cutoff in the comparisons presented in the next section.

IV. COMPARISON OF DIFFERENTIAL CROSS SECTIONS FOR DIFFERENT REACTIONS AND DIFFERENT FINAL STATES

A. (p,t) Data

Figures 4 and 5 show that the experimental (p,t) angular distributions peak at an angle slightly greater than 20°. These peak differential cross sections are plotted in Fig. 6. The calculated (p,t) angular distributions peak at an angle slightly less than 25°. The calculated peak differential cross sections are also plotted in Fig. 6. As described in Sec. II, these calculated cross sections are undefined to the extent of an over-all normalization constant. We have chosen this constant (the same for all cases) to produce the best visual fit between the calculations and the data. It is evident from Fig. 6 that our calculations give a reasonably good account of the ratios of the peak cross sections. The calculated systematics are influenced by variations in both nuclear-structure and nuclear-reaction aspects of the process. For example, the spectroscopic amplitudes

TABLE X. Calculated peak cross sections[a] (~25°) for pure $(nlj)^2$ transfer. (E_p=39.8 MeV.)

Reaction	Q (MeV)	$(1g_{9/2})^2$	$(2p_{1/2})^2$	$(1f_{5/2})^2$	$(2p_{3/2})^2$	$(1f_{7/2})^2$	$(1d_{3/2})^2$	$(2s_{1/2})^2$
$Ca^{42}(p,t)$	−11.35		28.1	5.5	76.9	12.4	4.1	23.3
$Ca^{48}(p,t)$	− 8.75		10.3	0.6	37.1	6.2	4.4	20.3
$Ni^{58}(p,t)$	−13.97	7.6	10.0	0.9	29.9	5.1		
$Ni^{64}(p,t)$	− 8.02	2.7	11.3	1.6	27.9	4.5		

[a] If the normalization constant in the DWBA program is chosen to give the best visual fit to the (p,t) data, then the unit used in this table is ~14 μb/sr.

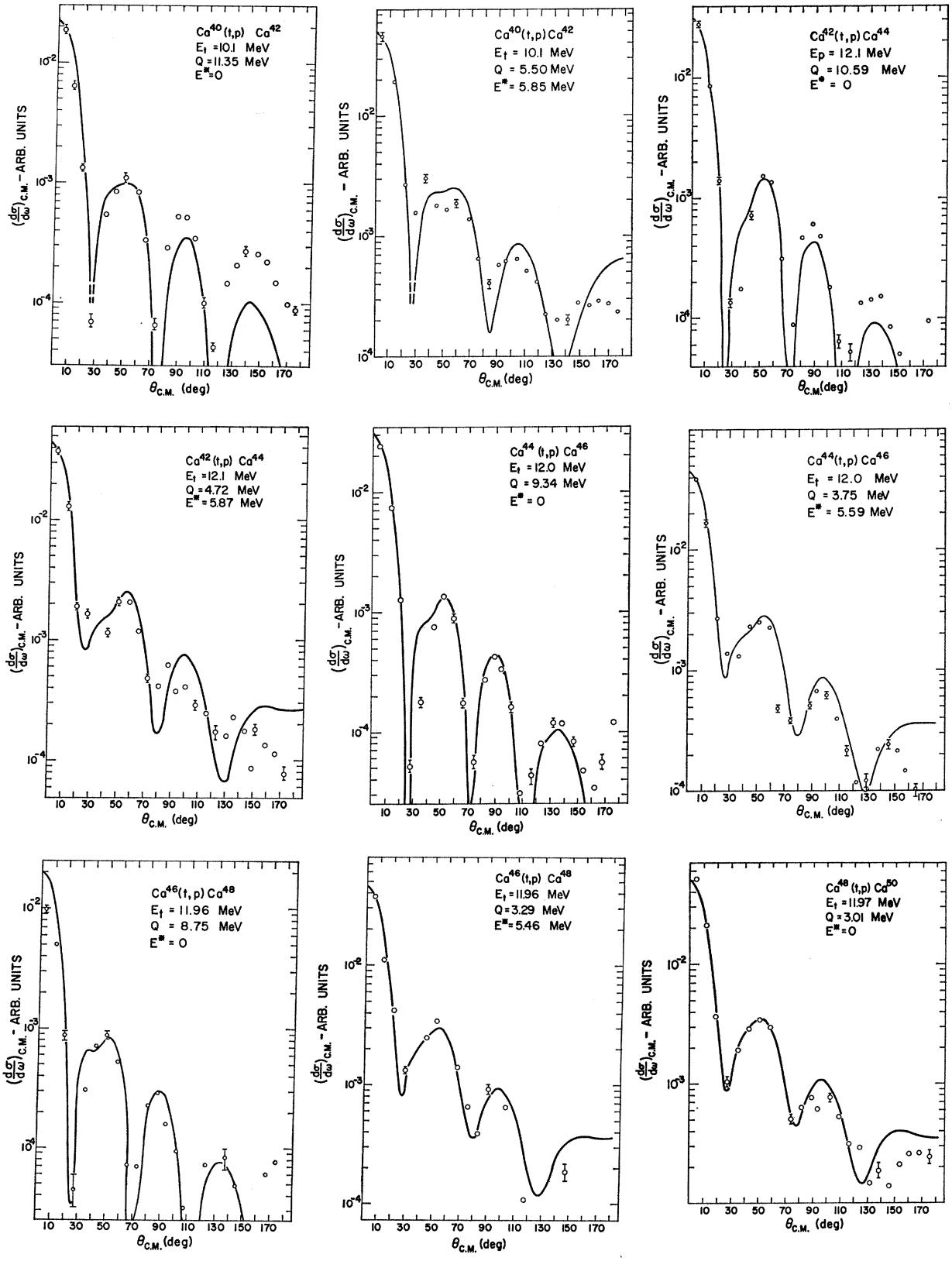

FIG. 3. Comparison between experimental (open circles) and calculated (solid line) angular distributions for the Ca(t,p) reactions. The data are from Ref. 1.

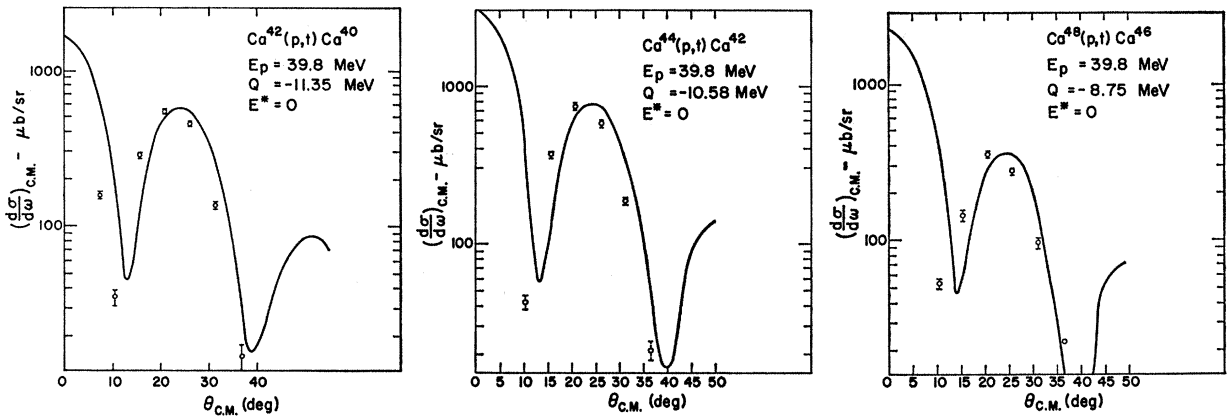

FIG. 4. Comparison between experimental (open circles) and calculated (solid line) angular distributions for the ground-state Ca(p,t) reactions. The data are from Ref. 2.

for the $Ca^{42}(p,t)$ and $Ca^{48}(p,t)$ ground-state transitions are very nearly equal (see Table VI). However, the smaller Q value of $Ca^{48}(p,t)$ implies a greater momentum mismatch, which results in a smaller cross section (see Table X), in agreement with experiment. On the other hand, the calculated $Ni^{58}(p,t)$ cross section is brought down to near equality with the $Ca^{42}(p,t)$ cross section by both nuclear-structure and nuclear-reaction con-

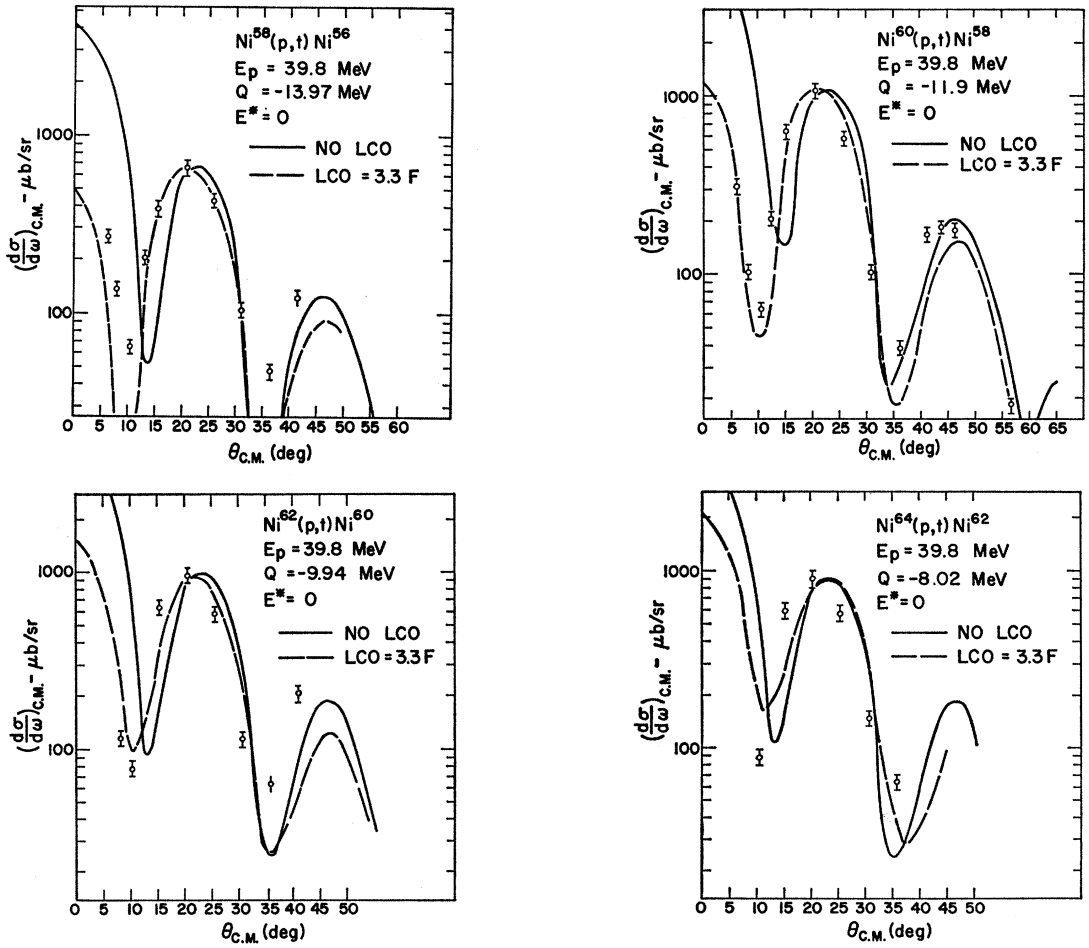

FIG. 5. Comparison between experimental (open circles) and calculated angular distributions for the ground-state Ni(p,t) reactions. The solid line is for no lower cutoff, and the dashed for a lower cutoff of 3.3 F, in the DWBA integral. The data are from Ref. 2.

siderations. It is seen in Table VIII that our calculation implies that an appreciable amount of $(1f_{5/2})^2$ transfer is involved in $Ni^{58}(p,t)$, enough so that the smallness of the $(1f_{5/2})^2$ reaction amplitude offsets the gain in cross section normally associated with coherence. In $Ca^{42}(p,t)$ the admixture of $(2p_{3/2})^2$ transfer augments the cross section both by virtue of its larger amplitude and the coherence.

B. (t,p) Data: Ground States

The experimental (t,p) angular distributions shown in Fig. 3 are given in arbitrary units, different units for each isotope. Thus we cannot use these data to compare experimental and calculated relative cross sections. The authors of Ref. 1 have presented the relative cross sections for the different ground-state transitions in terms of the sums of different cross sections at $\Theta_{lab}=5°$, 12.5°, and 20°, relative to the value of this sum for $Ca^{40}(t,p)Ca^{42}$. These sums are plotted in Fig. 7. We have also plotted in Fig. 7 our calculated differential cross section, summed for $\Theta_{c.m.}=5°$, 10°, 15°, and 20°, again with the normalization constant chosen to give the best visual fit. With the exception of $Ca^{40}(t,p)Ca^{42}$, the agreement between the data and the calculation is within quoted experimental errors. Q-value dependence and configuration mixing both conspire to weaken the $Ca^{48}(t,p)Ca^{50}$ ground-state transition relative to ground-state transitions between the lighter Ca isotopes. As was true in the (p,t) case, the relative strength of the transition between the Ca^{40} and Ca^{42} ground states was calculated to be too large. This is due in part to our failure to consider the excitation of protons out of the $2s_{1/2}$ and $1d_{3/2}$ shells. It is reasonable to expect that our Ca^{40} calculation suffers most from this neglect.

The (p,t) data we have considered involved center-of-mass proton energies of about 39 MeV. The center-of-mass proton energies for the (t,p) data were about 22 MeV. It is interesting to ascertain the extent to which our DWBA calculation can account for the influence of this energy difference on the differential cross sections. If the normalization constant in the DWBA calculation is determined from the (p,t) comparison of Fig. 6, then we predict that the 5° differential cross section in the $Ca^{44}(t,p)Ca^{46}$ ground-state transition should be 3.65 mb/sr. It is observed[1] to be 4.0 ± 1.0 mb/sr. Thus, within these rather wide limits of uncertainty, we have been able to account for all the ground-state data, both in (p,t) and (t,p), with a single normalization constant.

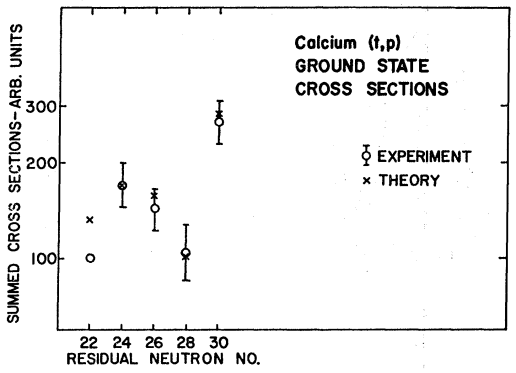

FIG. 6. Comparison of peak ground-state (p,t) experimental cross sections (open circles) with calculated values (crosses). A single over-all normalization constant has been chosen for the theoretical values. The data are from Ref. 2.

C. (t,p) Data: Excited 0^+ States

Reference 1 gives the strength of (t,p) transitions to excited states relative to the strength of the ground-state transition. The numbers compared are differential cross sections, summed over the angles $\Theta_{lab}=5°$, 12.5°, 20°, 32.5°, $\cdots$, 87.5°, or 177.5°. Table XI lists these ratios for the excited 0^+ states strongly populated in the reactions $Ca^{40\to46}(t,p)$, together with the energies of these states. Our calculation also predicts a strong transition in each of these cases. Our calculated energies and ratios of cross-section sums ($\Theta_{c.m.}=5°$, 10°, 15°, $\cdots$, 90°, or 175°) are also given in Table XI. Using $G=20/A$, we predict excited 0^+ cross sections which are too large, relative to the ground-state cross sections, by about a factor of 2. Either these excited 0^+ states involve degrees of freedom which cannot be expressed in terms of neutron seniority-zero component (e.g., deformation), or else the pairing force strength $G=20/A$ leads to an underestimate of the amount of configuration mixing. We have found that $G=27/A$ yields eigenvectors that are in better agreement with the observed ratio of excited-state intensities, and the relative cross sections for the ground-state transitions. Furthermore the values of V_j^2 calculated from $G=27/A$ (see Figs. 1 and 2) are in good agreement with single-particle trans-

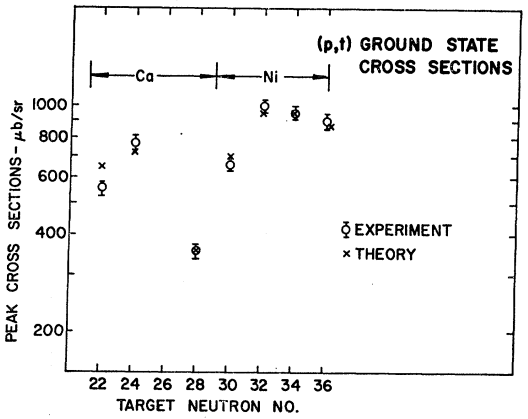

FIG. 7. Comparison of summed ground-state (t,p) experimental cross sections (open circles) with calculated values (crosses). A single over-all normalization factor has been chosen for the theoretical values. The data are from Ref. 1.

TABLE XI. Comparison of (t,p) reaction strengths leading to excited and ground states of the calcium isotopes.

	Experimental		Calculated $G=20/A$		Calculated $G=27/A$	
Final nucleus	E^* (MeV)	Ratio (exc./gnd.)	E^* (MeV)	Ratio	E^* (MeV)	Ratio (exc./gnd.)
Ca^{42} [a]	5.85	0.97	8.17	2.32	9.46	1.48
Ca^{44} [b]	5.86	0.81	8.39	1.58	9.25	1.02
Ca^{46} [b]	5.60	0.55	8.30	1.76	8.37	0.33
	5.63	0.37			8.70	0.81
Ca^{48} [b]	5.46	1.60	7.41	3.22	6.85	1.61
Ca^{50} [a]	4.47	~0.05	5.17	0.16	5.78	0.09

[a] Experimental transition strengths are expressed in terms of the differential cross section summed over the 24 angles 5°, 12.5°, 20°, ···, 177.5°. Calculated transition strengths are expressed in terms of the differential cross section summed over the 35 angles 5°, 10°, 15°, ···, 175°.

[b] As in (a), except that the sum of experimental differential cross sections extended over the 12 angles 5°, 12.5°, 20°, ···, 87.5°, and the sum over calculated cross section extended over the 18 angles 5°, 10°, 15°, ···, 90°.

fer data. Actually, the $G=27/A$ predictions give a slightly better fit to the data than do the $G=20/A$ predictions. However, a pairing force with strength $G=27/A$ overpredicts the odd-even mass differences by about 50%.

It is evident from Tables VII and X that the dominant feature of the (t,p) excitation of these strong 0^+ states is expected to be $(2p_{3/2})^2$ transfer. However, there is also some $(2p_{1/2})^2$ transfer that interferes constructively with it, since the spectroscopic amplitudes ($S_{p_{3/2}}\sim 0.94$, $S_{p_{1/2}}\sim 0.13$) have the same sign. Our calculation predicts a state several MeV higher which would be reached largely by $(2p_{1/2})^2$ transfer ($S_{p_{1/2}}\sim 0.9$, $S_{p_{3/2}}\sim -0.4$). Here the $2p_{1/2}$ and $2p_{3/2}$ spectroscopic amplitudes have opposite signs and interfere destructively. Thus we predict that most of the excited 0^+ strength should be concentrated in a single state. The weakness of the excited 0^+ transition in $Ca^{48}(t,p)Ca^{50}$ can also be understood in terms of this destructive interference.

In the case of $Ca^{44}(t,p)Ca^{46}$ the excited 0^+ strength is seen to be divided between two nearly degenerate 0^+ states (5.60 and 5.63 MeV). This occurrence is unexplained by our $G=20/A$ calculation. However, when we used the stronger pairing force $G=27/A$, we did find division of strength between two nearly degenerate excited 0^+ states in Ca^{46} (and only in this case). The extra state involved a large $d_{3/2}$-hole component.

V. DISCUSSION

Other workers[6,7,16] have reported more realistic shell-model calculations for the Ca and Ni isotopes than we have presented here. Some of these workers have used their calculated eigenstates to draw conclusions about (p,t) and (t,p) cross sections. In a sense, our calculation has been more ambitious, since we have attempted to relate data for both reactions, over a wide range of nuclei, taking at least semiquantitative account of effects involving nuclear structure and reaction dynamics. On the other hand, by limiting our attention to 0^+ states we have considered only a small part of the available data. We have found that (t,p) and (p,t) reaction data between the even Ca and Ni ground states are consistent with a picture of these states in terms of simple pairing degrees of freedom of the extra-core neutrons. It is now tempting to extend the range of our calculations to include other series of isotopes. Our simple picture also gives an approximate account of the occurrence of strong (t,p) transitions to 0^+ states in Ca^{42} through Ca^{48} at about 5.8 MeV. However, we overestimate the cross section for population of these states. This indicates that the real states also involve other, more complicated, degrees of freedom that are not simply related to the Ca ground states by the addition of a zero-coupled pair.

Finally, we note that the first excited 0^+ states in the even Ca isotopes, occuring at an excitation energy of about 2 MeV, are completely unrelated to the seniority-zero degrees of freedom we have included in our calculation. We find no Ca eigenvalues at such a low excitation energy. Furthermore, these states are populated very weakly in two-neutron transfer reactions.

[16] R. Broglia, P. Federman, Ole Hansen, F. Kehl, and C. Riedel (to be published); J. Vervier, Phys. Letters **22**, B2 (1966); T. Engeland and E. Osnes, *ibid.* **20**, 424 (1966); B. J. Raz and M. Soga, Phys. Rev. Letters **15**, 924 (1965); T. Komoda, Nucl. Phys. **51**, 234 (1964).